L. Bencsik, A. Zelei: Effects of human running cadence and experimental validation of the bouncing ball model, *Mech. Syst. Signal Process.* (2016), http://dx.doi.org/10.1016/j.ymssp.2016.08.001

Effects of human running cadence and experimental validation of the bouncing ball model

László Bencsik[*], Ambrus Zelei[†]

June 21, 2016

Highlights:

- The bouncing ball model is applied for the analysis of dynamic effects of cadence.
- Energy loss due to ground-foot collision and impact intensity are estimated.
- Based on the model, higher cadence imply lower energetic costs and lower risk of injury.
- Video-captured kinematic data of 121 amateur runners validated the model.
- Statistics for step length, cadence, and walk-to-run transition speed are provided.

[*]MTA-BME Research Group on Dnyamics of Machines and Vehicles, Muegyetem rkp. 3, Budapest, H-1111, Hungary, bencsik@mm.bme.hu (Corresponding author)

[†]MTA-BME Research Group on Dnyamics of Machines and Vehicles, Muegyetem rkp. 3, Budapest, H-1111, Hungary, zelei@mm.bme.hu

Abstract

The biomechanical analysis of human running is a complex problem, because of the large number of parameters and degrees of freedom. However, simplified models can be constructed, which are usually characterized by some fundamental parameters, like step length, foot strike pattern and cadence. The bouncing ball model of human running is analysed theoretically and experimentally in this work. It is a minimally complex dynamic model when the aim is to estimate the energy cost of running and the tendency of ground-foot impact intensity as a function of cadence. The model shows that cadence has a direct effect on energy efficiency of running and ground-foot impact intensity. Furthermore, it shows that higher cadence implies lower risk of injury and better energy efficiency. An experimental data collection of 121 amateur runners is presented. The experimental results validate the model and provides information about the walk-to-run transition speed and the typical development of cadence and grounded phase ratio in different running speed ranges.

Keywords: *biomechanics of running, vertical displacement, energy efficiency, ground-foot impact intensity, minimally complex dynamical model*

1 Introduction

Professional runners' training process involves the biomechanical analysis of their body motion. In contrast, amateur runners usually do not focus on the development of injury preventing and energy efficient running form. However, considerable improvement can be achieved by taking into consideration some basic biomechanical rules. A lot of materials from the Internet and magazines discuss the improvement of running style. However, these information are contradictory in many issues and they are mostly based on personal experience and not on thorough scientific investigation. Present work aims to contribute to the actual researches related to the understanding of the biomechanics of human running.

Many works like [1, 2] contribute to the thorough understanding of bipedal locomotion, human walking and running. Several approaches and organizations [3, 4, 5] have been developed which aim to gather and disseminate practical, science based knowledge about healthy, injury preventing, energy efficient and natural way of running. Researchers apply different type of biomechanical models of a wide range of complexity. A lot of complex high degree of freedom (DoF) mechanical models exist, which are suitable for motion capturing, dynamic and kinematic analysis of the human body and running motion carefully. However these investigations are hard to use for prediction regarding the effect of a parameter modification, due to the extremely large number of variables. However, in the case, when a specific issue is investigated, simplified dynamical models may be more predictive than a very complex, high DoF model with large number of parameters. Starting from the most complex models, e.g. [6] towards the simplest ones, we can mention some low DoF segmental models [7, 8, 9, 10] and some spring legged models [11, 12], besides many other examples.

The most fundamental parameters, with which the running form can be characterized, are running speed, step length, *step frequency* and strike pattern besides many other parameters. Many articles study the effect of step frequency also known as *cadence*, which indicates the average number of steps within one-minute-long time duration. The effect of cadence c is in the focus of this work, which is considered to be one of the most important parameters, when running form is analysed [13, 14, 15, 16, 17]. The bouncing ball model was introduced in [18], which is the simplest possible model for the investigation of the dynamic effects of cadence. Present work details an extended theoretical and experimental study of the bouncing ball model.

One can chose from infinite number of alternatives of step length s and cadence c value pairs at a certain running speed $v_x = s\,c$. It is demonstrated by the experiments explained in [13] that the optimal cadence, when the oxygen uptake (the indicator of physical loading of the body) is minimal, and the freely chosen convenient cadence are not the same for most of the people. Present work aims to find practical directives that helps the choice of proper cadence value.

Present paper aims to show that cadence has a direct effect on energy efficiency and ground-foot impact intensity by means of a simple dynamic model. The simple but still useful estimations are based on the dynamics of a bouncing ball.

The bouncing ball model of running is validated by measurements in [18] involving the measurement data of 41 people. Present work provides an extended experiment with 121 people and thorough mechanical and statistical analysis of the collected data. The effect of the ratio of the flight phase and the grounded phase is considered in this work, in contrast to [18], where zero grounded phase was assumed. In the present work we determined the flight phase value for which the bouncing ball model and the reality are the closest to each other. The results of [18] are extended by the model based estimation of the mechanical power which is absorbed by ground-foot collision. Besides, present analysis of the measured data confirmed the typical speed of walk-to-run transition that can be find in the literature.

2 Theoretical background

The bouncing ball model and its application for predicting energy efficiency and ground-foot impact intensity are detailed in this section.

2.1 The bouncing ball model

The mass of the body is shrunken into a single point mass m located in the centre of gravity (CoG) during flight phase. The model considers gravity and impulsive ground reaction force, while other external forces, like aerodynamic forces are neglected. The parabolic path of the CoG during flight phase is in the vertical (x-y) plane depicted in Fig. 1 left. We assume that the parabolic path is identical in each step, for which the necessary amount of energy is provided by the runner. The complete time period T of each step is separated into grounded phase T_{g} and flight phase T_{f} as the t-y plot in Fig. 1 right shows. Each parabolic segment with time duration T_{f} starts from the same location where the previous one ends, but time T_{g} passes between.

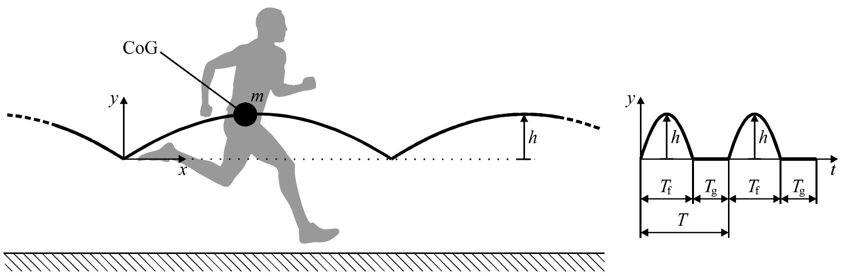

Figure 1: Idealized path of a runner's CoG (left), time history of the CoG vertical position.

The bouncing ball is a minimally complex model, which is suitable only for the investigation of the effects of cadence on the ground-foot impact intensity and the collision induced energy absorption. The model is limited to find approximate relation between cadence, vertical displacement amplitude of the CoG of the body and mechanical power consumption of running. Many kinematic and dynamic parameters are ignored, such as posture of the body during the gait cycle, strike pattern or flexibility of muscles, tendons and footwear.

The motion of the CoG during flight phase is described by the following kinematic equations:

$$x(t) = x_0 + \dot{x}_0 t, \tag{1}$$

$$y(t) = y_0 + \dot{y}_0 t - \frac{g}{2} t^2, \tag{2}$$

where x_0 and y_0 are the initial position coordinates while $\dot{x}_0$ and $\dot{y}_0$ are the initial velocity components represented in a Cartesian system (see: Fig. 1). The vertical velocity component is $\dot{y}(T_{\mathrm{f}}) = -\dot{y}_0$, right before point mass m collides with the ground at the end of the flight phase $t = T_{\mathrm{f}}$. Therefore the vertical pre-impact velocity can be expressed as the function of time duration T_{f} of the flight phase after time differentiating equation (2):

$$\dot{y}_0 = g\,T_\mathrm{f}/2. \tag{3}$$

Besides, we can apply the principle of conservation of mechanical energy. From that it is straightforward to determine the initial vertical velocity magnitude as the function of the height h of the parabolic path, if $y_0 = 0$:

$$\dot{y}_0 = \sqrt{2gh}. \tag{4}$$

Combining equations (3) and (4), we obtain the height h of the parabolic path as the function of the flight phase time duration T_f:

$$h = \frac{1}{8}\,g\,T_\mathrm{f}^2. \tag{5}$$

In order to make the bouncing ball model more accurate, we consider the ratio $r_\mathrm{f} = T_\mathrm{f}/T$ of the flight phase time duration T_f and the total time duration T of a step. Its typical value is in the range of $r_\mathrm{f} = 0.22 \ldots 0.6$ and higher values characterize professional, elite runners [2]. We also consider that the total time period T[s] of one step is in direct relation with cadence c which usually possesses [steps/min] unit in the literature, thus we can write that $T = 60/c$. Similarly, the time period T_f of the flight phase and cadence has the relation: $T_\mathrm{f} = 60\,r_\mathrm{f}/c$. Finally, the function which gives the relation between cadence and the height of the parabolic path is written as:

$$h = \frac{450\,g\,r_\mathrm{f}^2}{c^2}. \tag{6}$$

The path of the CoG during flight phase is depicted in Fig. 2 in case of different cadence values for flight phase ratio $r_\mathrm{f} = 0.67$, which is originated from the experimental results (to be explained in the subsequent sections). The height of the parabolic path predicted by the bouncing ball model is visualized by thick solid lines in Fig. 3 for different flight phase ratios. The following subsection explains that the parabola height, which is defined by (6), is directly proportional to the impact intensity I_{Fy}. It will be also explained later that h is in relation with the energy absorption due to ground-foot impacts. The experimental data in Fig. 3 and its statistic analysis are also explained in the subsequent sections.

2.2 Impact intensity and energy efficiency

Again, the relation between the parabola height h and the vertical velocity component $\dot{y}_0$ right before the impact is given by (4). It is demonstrated by [8] and [19] that the impact forces correlate with the kinetic energy content which is absorbed due to the foot impact. It is called *constrained motion space kinetic energy* (CMSKE) in the literature. CMSKE is directly proportional to the impulse of the contact reaction

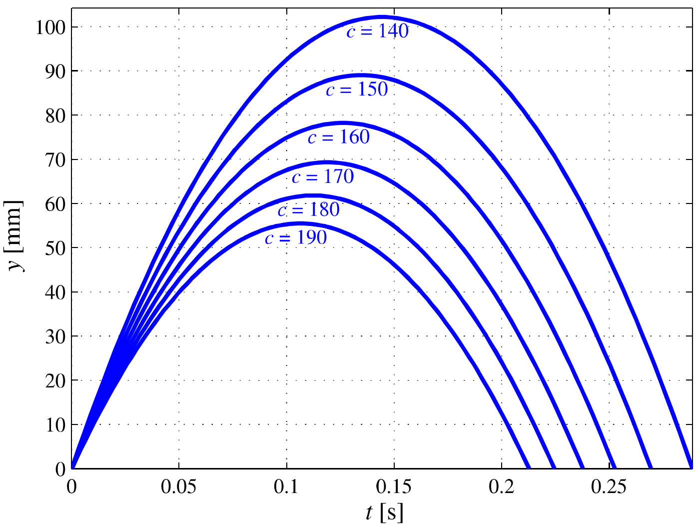

Figure 2: Parabolic path of CoG during flight phase for $r_\mathrm{f} = T_\mathrm{f}/T = 0.67$ ($c = 140...190$ [steps/min]).

force and also to the peak reaction force [8, 20]. The related effective mass concept for foot impact is introduced in [21] for a one DoF model. The cited studies have shown that foot strike intensity can be characterised by the CMSKE which depends on the pre-impact configuration and velocity and the effective mass matrix. Summarizing, lower vertical pre-impact velocity leads to smaller impact intensity in case of the bouncing ball model.

Since, the motion of the bouncing ball in the vertical direction is constrained by the ground, CMSKE is calculated from the vertical pre-impact velocity component:

$$E_\mathrm{c} = \frac{1}{2} m \dot{y}_0^2. \tag{7}$$

We express $\dot{y}$ from (4) and then we substitute into equation (7) which gives the well known formula: $E_\mathrm{c} = mgh$. This formula shows that all of the potential energy of level h is absorbed by ground-foot impact at the end of the flight phase. The main message is that the impact intensity is in linear relation with the maximum vertical displacement of the body. After that we express h from (6) as a function of cadence and substitute into the (7) expression of E_c and we gain:

$$E_\mathrm{c} = \frac{450\, m\, g^2\, r_\mathrm{f}^2}{c^2}. \tag{8}$$

Equation (8) gives CMSKE, which is absorbed due to the impact in every foot strike. This mechanical energy content must be provided by the muscles in each step.

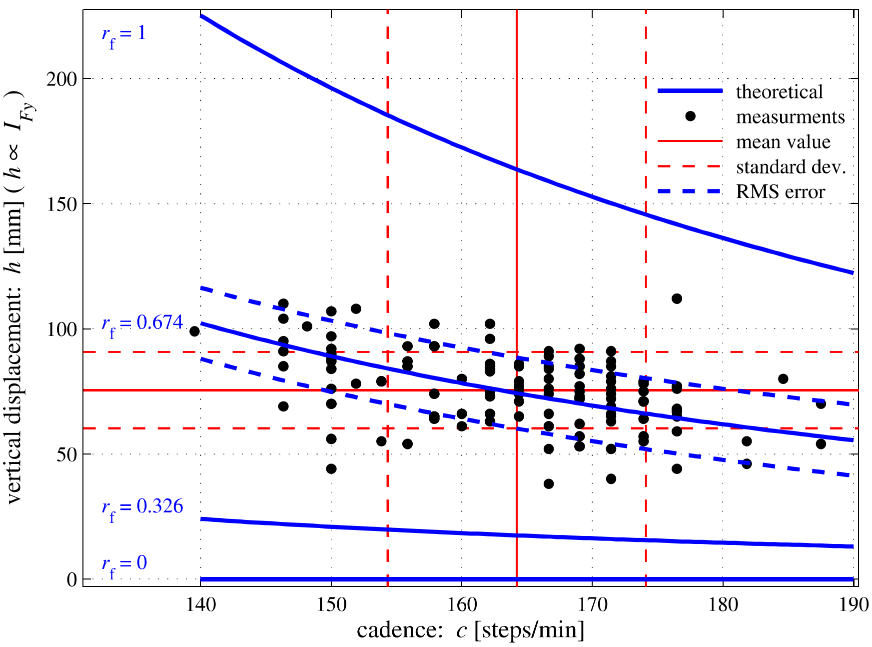

Figure 3: Theoretical and experimental results for vertical displacement h.

An average mechanical power P_c is calculated that covers CMSKE in every foot strike (see (9)). P_c related to CMSKE is shown in Fig. 4 as a function of cadence c for an $m = 80\,\text{kg}$ bodyweight person in case of different flight phase ratios (r_f). The plotted values are within the range of mechanical power which is presented in [22].

$$P_c = \frac{7.5\, m\, g^2\, r_f^2}{c}. \tag{9}$$

Comparing the resulting formula (8) to CMSKE and equation (6), one can conclude that E_c is directly proportional to h. Hence, the impact intensity I_{Fy} is also directly proportional to the vertical displacement h ($I_{Fy} \propto h$). Therefore, the measured values characterize the impact intensity in Fig. 3. The impact intensity is interpreted by the impulse I_{Fy} of the vertical component of the contact force F_y, which is obtained by integrating it on the time duration of the impact:

$$I_{Fy} = \int F_y \, \mathrm{d}t. \tag{10}$$

Finally, considering (6) and the direct proportionality of I_{Fy} and h, we can con-

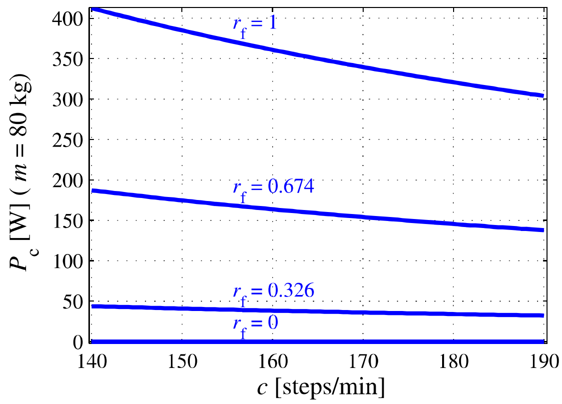

Figure 4: Power P_c related to CMSKE.

clude that the impact intensity is directly proportional to the reciprocal function of the square of the cadence:

$$I_{Fy} \propto \frac{1}{c^2}, \tag{11}$$

based on the bouncing ball model.

Equations (9) and (11) show that zero energy cost and zero impact intensity could be achieved with infinitely high step frequency ($\lim_{c\to\infty} P_c = 0$ and $\lim_{c\to\infty} I_{Fy} = 0$). These statements can be confirmed by extending the graphs in Fig. 3. Infinitely high cadence is obviously not feasible in reality. The optimal stride frequency is limited by the muscular activity which depends on the stretch-shortening cycle of the muscles, which is not included in the model. Nevertheless, the model predicts that higher cadence should be kept in order to achieve better energy efficiency and lower risk of impact induced injury.

3 Experimental method

In order to prove the validity of the bouncing ball model an experiment was accomplished, in which the motion of 121 runners was video-captured. Every investigated person was amateur runner at the age from 15 to 50 and from both sex. The measured people were told to run a distance of 4 km with a convenient speed on an open air running track. Their motion was recorded on a 5 m long distance by a high resolution video camera before the end of the 4 km run. The speed of the camera was 50 frames/s and its resolution was 1920 × 1080 pixels.

The foot landing position and the vertical elevation h (peak-to-peak) of the head was registered based on the video frames. The vertical displacement h of the head gives an acceptable estimation of the vertical displacement of the CoG of the body, although reference [23] provides a comparison of methodologies and the results of a large scale data experiment which aims to measure the vertical displacement of runners. Besides, the time duration T between foot strikes, and flight phase time duration T_{f} were determined. The measured parameters are listed in the Appendix A in Table 2: running speed v_x, step length s, cadence c, peak-to-peak vertical displacement h and flight phase ratio r_{f}. The grounded phase ratio $r_{\mathrm{g}} = 1 - r_{\mathrm{f}}$ was calculated for each runner. The mean values and standard deviation values are collected in Table 1.

The speed v_x of each person was determined by measuring the time duration needed to take a specified distance. However an alternative possibility is to calculate the speed based on the cadence and step length data. The difference between the average v_x and $s\,c$ is 0.39% and the standard deviation is quite close to each other, which shows the reliability of the velocity, step length and cadence measurement.

Table 1: Mean value, standard deviation and uncertainty interval (at the level of confidence of 95%) of the measured data: running speed v_x, step length s, cadence c, peak-to-peak vertical displacement of the head h, flight phase ratio r_{f} and grounded phase ratio r_{g}.

	v_x km/h	s m	c 1/min	$s\,c$ km/h	h mm	r_{f} -	r_{g} -
mean value	9.83	0.993	164.2	9.79	75.5	0.326	0.674
standard deviation	1.70	0.156	9.89	1.69	15.3	0.0801	0.0801
measurement uncertainty	±0.25	±0.02	±2	±0.23	±6	±0.02	±0.02

4 Experimental results and validation of the bouncing ball model

In order to validate the bouncing ball model, the measured cadence and height data are indicated by dots in Fig. 3 together with the theoretical curves. The measured vertical displacement data are slightly under the measured values in [24]. The mean value and the standard deviation of the cadence c and peak-to-peak vertical displacement h is plotted by solid and dashed thin lines respectively. The theoretical $h(c)$ curve described by equation (6) is plotted with four different flight phase ratio values with solid thick lines. The $r_{\mathrm{f}} = 1$ case is quite far from the measured points, which means that the bouncing model does not fit quantitatively to the reality without considering the grounded phase. However, qualitatively good coherence can be observed between the measured data and the theoretical curve. A simply theoretical case is

$r_{\mathrm{f}} = 0$, when the flight phase and therefore the parabolic path disappears and the bouncing ball model predicts zero vertical movement.

The mean value of the measured flight phase ratios is $r_{\mathrm{f}} = 0.326$ (see: Table 1) for which the theoretical curve still does not fit very well, however it fits to the measurements qualitatively. Still, the measured displacements are larger than the theoretically predicted value. The bended leg enables vertical movement in the grounded phase. This is the possible reason for the gap between the theoretical and experimental results. For the investigation of this phenomenon many scientific results are available, e.g. [11, 12].

The theoretical curve and the measured results fit the best for $r_{\mathrm{f}} = 0.674$. The root-mean-square deviation is $RMS_{h(c)} = 14.2\,\mathrm{mm}$ which is 18.8% if it is normalized by the mean value of h. The RMS deviation is represented by thick dashed lines. The correction of the r_{f} value enables us to rely on the bouncing ball model.

As a secondary result, the measurements confirmed that the investigated runners tend to chose a larger stride length and they do not change the cadence, when they are running in different speed as it is illustrated by Fig. 5 and Fig. 6. The measured values are indicated by dots in both figures. The mean values of speed, cadence and step length are shown by thin solid lines while the dashed thin lines represent the standard deviation. Linear function was fit to the experimental results in both cadence versus speed and step length versus speed cases. The best fit linear for cadence is $c = 142.4 + 2.215 v_x$ (c is given in [steps/min] and v_x is given in [km/h] unit) and the RMS deviation is $RMS_{c(v)} = 9.1469\,\mathrm{steps/min}$ (the RMS deviation normalized by the mean value of c is 5.57%). The best fit linear for step length is $s = 0.153 + 0.0854 v_x$ (s is given in [m]) and the RMS deviation is $RMS_{s(v)} = 0.0571\,\mathrm{m}$ (the RMS deviation normalized by the mean value of s is 5.75%). The best fit lines show that much higher steepness characterizes step length than cadence. The correlation between measured speed and cadence values is $\rho_c = 0.3810$, but a much higher value, $\rho_s = 0.9307$ characterizes the speed and step length pair. To sum up, the running speed is mainly set by changing the step length and not by the cadence in case of the examined people.

Fig. 7 shows the relation of speed and the grounded phase ratio. The experimental data represented by black dots show hyperbolic shape. The best fit hyperbolic function was find in the form: $r_{\mathrm{g}} = 3.08/v_x + 0.351$. The RMS deviation $RMS_{g(v)} = 0.0583$ is quite small, which is 8.65% using normalization by the mean value of r_{g}. The best fit hyperbolic curve is plotted by solid thick curve, and the RMS deviation is shown by the thick dashed lines. The mean values and the standard deviations of the experimental data are shown by solid and dashed thin lines respectively. The walk-to-run transition point (W-R) was defined using the extrapolation of the best fit hyperbolic curve. The W-R point, where the grounded phase ratio becomes

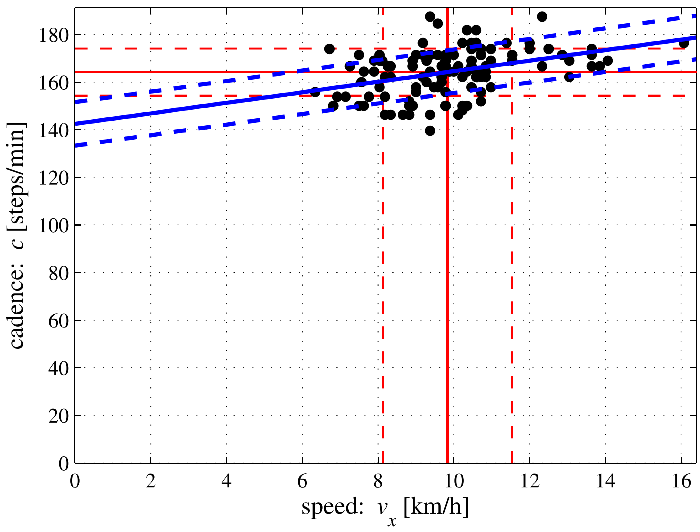

Figure 5: Cadence (c) versus running speed (v_x): measured data and the best fit line.

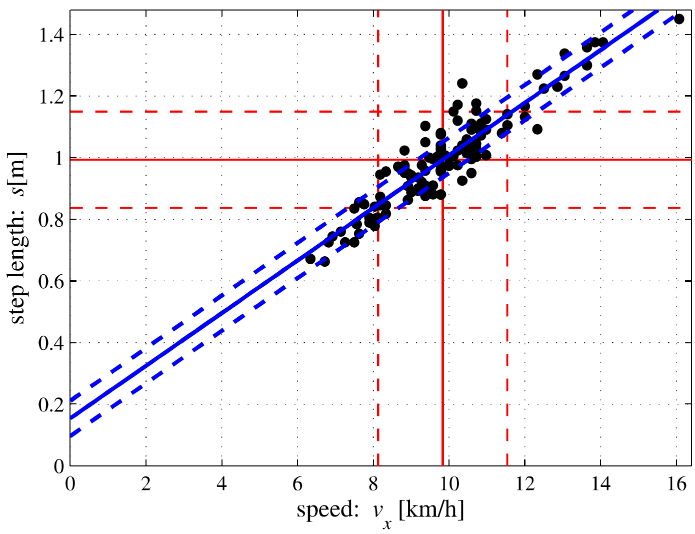

Figure 6: Stride length (s) versus running speed (v_x): measured data and the best fit line.

$r_\mathrm{g} = 3.08/v_x + 0.351 = 1$ is marked by the middle larger square. Here the speed is 4.74 km/h, while the smaller squared markers represent the RMS values at 4.35 km/h and 5.21 km/h speed, when $r_g \pm RMS_{g(v)} = 1$. This result is close to the literature results about walk-to-run transition speed [25].

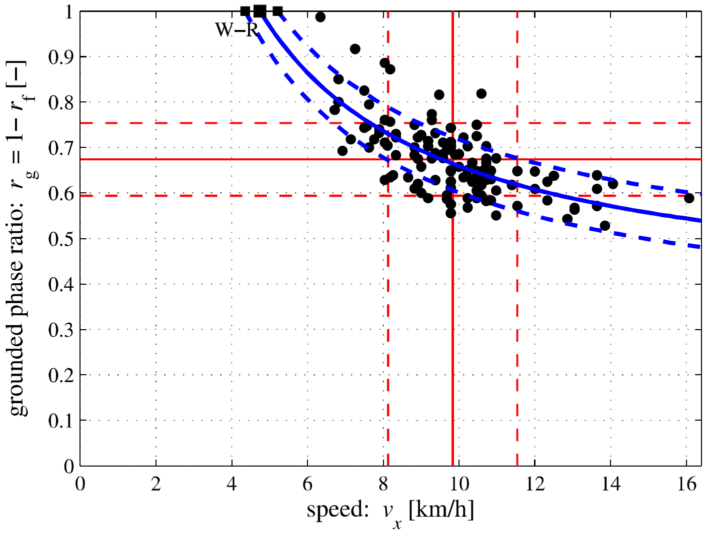

Figure 7: Grounded phase ratio (r_g) versus running speed (v_x): measured data and the best fit hyperbole.

5 Conclusions

The bouncing ball model was proposed, which is a minimally complex dynamic model when cadence and its effect on ground-foot impact intensity and energy efficiency of running are studied. The model exploits that the centre of gravity of the body moves on a parabolic path during the flight phase and the height of this parabolic path is determined by the cadence. The otherwise very complex multibody model of the human body was simplified to a single point mass, therefore the model has substantial limitations, e.g. the posture of the body cannot be involved into the analysis and the upper limit of physically feasible cadence value cannot be estimated.

According to the model, the elevation of the centre of gravity is directly proportional to the impact intensity, characterized by the impulse of the ground-foot contact force. The model indicates that the energy cost of running is a reciprocal function of cadence and the ground-foot impact intensity is a reciprocal function of the square of cadence. Summarizing, the higher the cadence is, the smaller the impact intensity and the energy cost are.

A large scale experimental data was collected in order to confirm the validity of the bouncing ball model. The kinematic data of 121 runners were collected by means of video capturing during long distance running. The flight phase ratio $r_\mathrm{f} = 0.674$ was found when the theoretical curve for the vertical displacement as the function of cadence fits the best to the measurement results. The normalized root-mean-square deviation is 18.8% which shows a moderately good fit of the measured data and theoretical curve. As a secondary result, the measurements showed that the correlation of step length and running speed is much larger than the correlation of cadence and speed. It means that people tends to change their step length rather than cadence when the running speed is varied. The experiments also showed that the grounded phase ratio is a hyperbolic function of speed. Furthermore, the estimated value of the walk-to-run transition speed matches with the available literature results.

The model verified that higher cadence is preferable, when the development of energy efficient and injury preventing running form is in focus.

Appendix A

Table 2: Measured data of 121 people: running speed v_x, step length s, cadence c, vertical displacement h.

no.	v_x km/h	s m	c 1/min	h mm	r_f –
1	16.1	1.45	176	65	0.41
2	13.6	1.3	167	80	0.36
3	9.4	0.9	171	52	0.31
4	9.2	0.9	176	76	0.41
5	9.8	0.975	167	74	0.39
6	9.4	0.875	188	70	0.31
7	9.8	0.96	167	66	0.44
8	9.4	0.91	171	74	0.37
9	11	1.125	158	93	0.39
10	8.8	0.975	150	88	0.3
11	13.6	1.3	171	91	0.43
12	10.6	1.11	162	96	0.41
13	7.5	0.725	171	63	0.26
14	9.6	0.91	171	40	0.31
15	10.2	0.975	176	59	0.41
16	9.7	0.99	162	86	0.41
17	6.8	0.725	150	56	0.2
18	6.8	0.725	150	44	0.15
19	13.8	1.375	167	91	0.47
20	9.8	0.88	171	85	0.26
21	9.8	1.08	150	92	0.43
22	12.3	1.27	167	76	0.42
23	8	0.8	171	52	0.11
24	8.8	0.97	150	76	0.25
25	8.3	0.845	162	73	0.27
26	8.2	0.945	146	104	0.37
27	10.6	0.95	182	46	0.18
28	9.4	1.05	146	85	0.27
29	9.5	1	158	65	0.18
30	7.3	0.725	167	38	0.08
31	10.3	0.925	182	55	0.33
32	9.8	1.075	150	107	0.38
33	7.5	0.835	150	70	0.18
34	9.6	0.995	158	64	0.29
35	11.5	1.105	171	69	0.43
36	9.7	0.99	162	85	0.41
37	8	0.79	171	66	0.37
38	10.6	0.995	176	44	0.38
39	11.4	1.08	176	68	0.38
40	12.9	1.23	171	87	0.46
41	7.6	0.855	150	70	0.3
42	8.7	0.971	146	91	0.37
43	10.7	1.045	171	65	0.37
44	8.3	0.852	167	84	0.36
45	9	0.888	171	81	0.4
46	8.3	0.955	146	69	0.32
47	8.3	0.818	167	61	0.28
48	12	1.132	176	67	0.35
49	7.1	0.76	154	79	0.28
50	10.8	1.083	167	76	0.42
51	10.7	1.096	162	83	0.3
52	9.2	0.936	162	66	0.3
53	10	0.973	171	76	0.31
54	10.2	1.172	150	97	0.35
55	9.4	1.103	140	99	0.37
56	10.3	1.241	150	90	0.38
57	12.3	1.092	188	54	0.38
58	10.7	1.003	171	72	0.34
59	8.8	1.023	146	95	0.39
60	10.6	1.016	176	77	0.35
61	10.5	1.059	158	93	0.39
62	10.2	1.023	162	84	0.3
63	9.8	1.04	150	87	0.35
64	8.9	0.949	150	84	0.33
65	10.1	1.15	146	110	0.37
66	8	0.841	158	74	0.29
67	8.2	0.846	162	63	0.24
68	10.3	1.04	164	74	0.37
69	9.8	1.016	164	74	0.29
70	10.1	1.005	167	61	0.28
71	10.5	1.029	169	72	0.35
72	10.7	1.152	156	87	0.32
73	11.5	1.141	169	82	0.35
74	10.7	1.03	171	79	0.34
75	7.6	0.784	160	66	0.25
76	9.4	0.958	164	76	0.32
77	6.7	0.663	174	75	0.22
78	10.7	1.026	174	55	0.33
79	10.5	1.015	174	64	0.28
80	8.8	0.951	152	78	0.32
81	7.6	0.753	164	65	0.21
82	7.9	0.805	164	77	0.26
83	7.9	0.789	169	53	0.27
84	8.9	0.863	169	62	0.38
85	9.3	0.903	169	75	0.32
86	9.8	1.028	156	93	0.3
87	9.9	1.007	164	79	0.32
88	7.8	0.849	154	79	0.28
89	9.7	0.998	160	80	0.41
90	10.8	1.111	162	75	0.35
91	10.6	1.091	164	85	0.37
92	14.1	1.374	169	92	0.38
93	13.6	1.358	174	71	0.39
94	9	0.943	156	85	0.27
95	10	0.979	164	71	0.34
96	8.2	0.873	154	55	0.13
97	9	0.936	158	102	0.34
98	9.3	0.921	169	53	0.24
99	10.5	1.051	167	85	0.25
100	12	1.167	174	57	0.39
101	12.5	1.224	174	78	0.36
102	11	1.091	169	57	0.32
103	10.7	1.176	152	108	0.42
104	13	1.265	169	85	0.44
105	13	1.338	162	102	0.43
106	10.5	1.044	176	112	0.41
107	8.9	0.908	167	52	0.28
108	11	1.008	174	71	0.45
109	8.1	0.806	169	88	0.3
110	9.8	0.959	169	73	0.35
111	6.9	0.744	154	79	0.31
112	9.2	0.892	171	76	0.29
113	9.7	1.002	167	89	0.31
114	10.2	1.12	148	101	0.43
115	10.7	1.005	174	79	0.36
116	9.8	0.955	169	72	0.3
117	9.3	0.976	160	61	0.23
118	8	0.778	169	77	0.24
119	6.3	0.671	156	54	0.01
120	10.8	1.072	164	86	0.37
121	9.6	0.881	185	80	0.32

Acknowledgments

This research has been supported by the Hungarian Scientific Research Fund, Hungary (Project Identifier: K-105433) and by the MTA-BME Research Group on Dynamics of Machines and Vehicles. These supports are gratefully acknowledged.

References

[1] W. Blajer, W. Schiehlen, Walking without impacts as a motion/force control problem, Journal of dynamic systems, measurement, and control 114 (4) (1992) 660–665.

[2] T. F. Novacheck, The biomechanics of running, Gait and Posture 7 (1998) 77–95.

[3] Chi Running official homepage, www.chirunning.com, last accessed: Aug. 2015 (2015).

[4] Natural Running Center official homepage, www.naturalrunningcenter.com, last accessed: Aug. 2015 (2015).

[5] Newton Running official homepage, www.newtonrunning.com, last accessed: Aug. 2015 (2015).

[6] K. Mombaur, A.-H. Olivier, A. Crétual, Forward and inverse optimal control of bipedal running, Modeling, Simulation and Optimization of Bipedal Walking 18 (2008) 165–179, volume 18 of the series Cognitive Systems Monographs.

[7] D. E. Lieberman, M. Venkadesan, W. A. Werbel, A. I. Daoud, S. D'Andrea, I. S. Davis, R. O. Mang'Eni, Y. Pitsiladis, Foot strike patterns and collision forces in habitually barefoot versus shod runners, Nature, Biomechanics 463 (7280) (2010) 531–535.

[8] J. Kövecses, L. Kovács, Foot impact in different modes of running: mechanisms and energy transfer, Procedia IUTAM 2 (Symposium on Human Body Dynamics, 2011) 101–108.

[9] A. Zelei, L. Bencsik, L. L. Kovács, G. Stépán, Impact models for walking and running systems - angular moment conservation versus varying geometric constraints, in: Z. Terze (Ed.), ECCOMAS Multibody Dynamics 2013, Book of Abstracts, Zagreb, Croatia, 2013, pp. 47–48, iSBN: 978-953-7738-21-1.

[10] A. Zelei, L. Bencsik, L. L. Kovács, G. Stépán, Energy efficient walking and running - impact dynamics based on varying geometric constraints, in: 12th

Conference on Dynamical Systems Theory and Applications, Lodz, Poland, 2013, pp. 259–270.

[11] M. Srinivasan, P. Holmes, How well can spring-mass-like telescoping leg models fit multi-pedal saggital-plane locomotion data?, Journal of Theoretical Biology 255 (1) (2008) 1–7, doi:10.1016/j.jtbi.2008.06.034.

[12] A. Merker, D. Kaiser, M. Hermann, Numerical bifurcation analysis of the bipedal spring-mass model, Physica D: Nonlinear Phenomena 291 (15) (2015) 21–30.

[13] E. Duverney-Guichard, J. V. Hoecke, The effect of stride frequency variation on oxygen uptake and muscular activity in running, Journal of Biomechanics 27 (6) (1994) 661–661, abstract of the XIVth ISB congress, doi:10.1016/0021-9290(94)90963-6.

[14] J. Hamill, T. R. Derrick, K. G. Holt, Shock attenuation and stride frequency during running, Human Movement Science 14 (1) (1995) 45–60, doi:10.1016/0167-9457(95)00004-C.

[15] C. T. Farley, O. González, Leg stiffness and stride frequency in human running, Journal of Biomechanics 29 (2) (1996) 181–186, doi:10.1016/0021-9290(95)00029-1.

[16] L. Li, E. C. H. van den Bogert, G. E. Caldwell, R. E. A. van Emmerik, J. Hamill, Coordination patterns of walking and running at similar speed and stride frequency, Human Movement Science 18 (1) (1999) 67–85, doi:10.1016/S0167-9457(98)00034-7.

[17] J. Morin, P. Samozino, K. Zameziati, A. Belli, Effects of altered stride frequency and contact time on leg-spring behavior in human running, Journal of Biomechanics 40 (15) (2007) 3341–3348, doi:10.1016/j.jbiomech.2007.05.001.

[18] L. Bencsik, A. Zelei, A study on the effect of human running cadence based on the bouncing ball model, in: 13th International Conference on Dynamical Systems Theory and Applications, December 7-10, 2015, Lodz, Poland.

[19] J. M. Font-Llagunes, R. Pamies-Vila, J. Kövecses, Configuration-dependent performance indicators for the analysis of foot impact in running gait, in: ECCOMAS, Multibody Dynamics 2013, Book of Abstracts.

[20] J. Kövecses, J. M. Font-Llagunes, An eigenvalue problem for the analysis of variable topology mechanical systems, ASME Journal of Computational and Nonlinear Dynamics 4 (3) (2009) 9 pages, doi:10.1115/1.3124784.

[21] K. J. Chi, D. Schmitt, Mechanical energy and effective foot mass during impact loading of walking and running, Journal of Biomechanics 38 (2005) 1387–1395.

[22] J. C. Sprott, Energetics of walking and running, Tech. rep., Physics Department, University of Wisconsin (Accessed: March 20, 2016).

[23] L. Gullstrand, K. Halvorsen, F. Tinmark, M. Eriksson, J. Nilsson, Measurements of vertical displacement in running, a methodological comparison, Gait & Posture 30 (1) (2009) 71–75, doi:10.1016/j.gaitpost.2009.03.001.

[24] J. S. Slawinski, V. Billat, Difference in mechanical and energy cost between highly, well, and nontrained runners., Med Sci Sports Exerc 36 (8) (2004) 1440–1446.

[25] F. J. Diedrich, W. H. W. Jr, Why change gaits? dynamics of the walk-run transition, Journal of Experimental Psychology: Human Perception and Performance 21 (1) (1995) 183–202.